

Methane dehydrogenation and aromatization over 4 wt% Mn/HZSM-5 in the absence of an oxidant

P.L. Tan,^{a,b} C.T. Au,^a and S.Y. Lai^{a,*}

^aDepartment of Chemistry and Centre for Surface Analysis and Research, Hong Kong Baptist University, Kowloon Tong, Hong Kong

^bSchool of Chemical Engineering, Wuhan University of Technology, Wuhan city, Hubei, 430070, P.R. China

Received 6 August 2006; accepted 10 October 2006

Methane dehydrogenation and aromatization over 4 wt% Mn/HZSM-5 in the absence of an oxidant (GHSV = 1600 mL h⁻¹ g⁻¹) was investigated. Mn/HZSM-5 was prepared by impregnation of HZSM-5 with manganese acetate tetrahydrate solution; Mn₃O₄ formed was the precursor of active phase for methane activation. The induction period over Mn/HZSM-5 catalyst before aromatic products appear was long at 700 °C. This period shortened with a rise of the reaction temperature to 800 °C. XPS and TPO results showed that the partly carburized or carburized Mn species formed are probably responsible for methane activation.

KEY WORDS: methane aromatization; Mn/HZSM-5; active phase.

1. Introduction

In the past decade, researchers have been searching for new effective catalysts for methane aromatization other than Mo/HZSM-5. The catalytic performance of Mo/MCM-22 catalyst was found to be comparable with that of Mo/HZSM-5 [1]. Besides Mo, transition metal ions (TMI), such as Fe, V, W and Cr, can also modify HZSM-5 zeolite [2] for the selective conversion of methane to C₂-hydrocarbon and aromatic compounds, although catalytic performances are usually lower than that of Mo/HZSM-5 catalyst. Rather than the carbides, the suboxides located on the external surface of zeolite were proposed as the active phases of all the TMI-modified HZSM-5 for methane activation. Zn/ZSM-5, an active catalyst for paraffin aromatization was also found to be active for methane activation [3]. In addition, Inui *et al.* [4] reported that methane could be converted to aromatic compounds (benzene and toluene) over Pt/H-Ga-Silicates catalyst prepared by means of rapid crystallization. Methane conversion of 4.2% and an aromatics selectivity of over 90% were obtained at 700 °C.

It was reported that manganese species exhibited good performance in methane oxidative coupling reaction [5]. It was also reported that MnO_x supported on silica and silica-alumina can catalyzed the transformation of methane to higher hydrocarbons in the absence of oxygen, showing that manganese oxide can activate methane [6]. Li *et al.* found that with Mn²⁺ ion-exchanged into HZSM-5, the performance of MoO₃/

MHZSM-5 for methane aromatization is enhanced by the suppression of deactivation [7]. However, research work on methane aromatization over Mn/HZSM-5 has never been conducted. In this work, methane aromatization over Mn-modified HZSM-5 in the absence of an oxidant was studied to determine whether an active and stable catalyst can be obtained. To elucidate the nature of the active phase on the Mn/HZSM-5 catalyst the catalyst was characterized by XPS and TPO and the processes of catalyst activation was studied by TPSR.

2. Experimental

2.1. Catalyst preparation

The 4 wt% Mn/HZSM-5 catalyst was prepared by impregnating HZSM-5 (SiO₂/Al₂O₃ = 50, Nankai University, P. R. China) with the required amount of manganese acetate tetrahydrate in aqueous solution at room temperature for 30 h. The catalyst was then dried at 120 °C for 6 h and calcined at 500 °C in air for 5 h. The calcined sample was crushed and sieved to 20–40 mesh for catalytic evaluation. The prepared catalysts were examined by infrared spectroscopy and no dealumination of the HZSM-5 was evident.

2.2. Catalyst evaluation

Catalytic reactions were carried out at atmospheric pressure in a continuous fixed-bed quartz micro-reactor (i.d. 4 mm) packed with 0.5 g catalyst. After the catalyst was pretreated in helium (25 mL min⁻¹) at 700 °C for 30 min, pure methane was introduced into the reactor

*To whom correspondence should be addressed.

E-mail: laisy@hkbu.edu.hk

through a Brooks mass flow controller for reaction at the required temperature. The reaction mixtures were analyzed on-line by gas chromatography using a column containing 5% Bentone 34 on Chromosorb W-AW for the separation of aromatic products and a HayeSep D column for the separation of CH_4 , CO , CO_2 , and other light hydrocarbons. The reactor outlet pipeline and the gas sampling valves were kept at a temperature above $160\text{ }^\circ\text{C}$ for effective sampling of all the aromatic products. Methane conversion and carbon-containing product selectivity were calculated on a carbon number basis.

2.3. Catalyst characterization

The decomposition of catalyst precursor was studied using a Perkin Elmer TG6 thermogravimetric analyzer and a Perkin Elmer DTA7 differential thermal analyzer. An uncalcined Mn/HZSM-5 sample was prepared by impregnating HZSM-5 with the required amount of manganese acetate tetrahydrate in aqueous solution at room temperature for 30 h and then dried at $50\text{ }^\circ\text{C}$. An 8 mg sample was used for the thermogravimetric analysis (TG) and a 20 mg sample was for the differential thermal analysis (DTA) experiment. The samples were heated from 30 to $900\text{ }^\circ\text{C}$ at a rate of $10\text{ }^\circ\text{C min}^{-1}$ in a stream of air of flow rate 20 mL min^{-1} . For comparison, manganese acetate tetrahydrate (MTA) was also analyzed under the same condition.

XPS spectra were acquired with an ESCALAB MK-II spectrometer (Al-K α : 1486.6 eV , 15 mA and 15 kV). The Si 2p line at 102.8 eV was taken as references for BE calibration. The used sample was cooled to room temperature quickly after reaction and kept in helium until introduction into the spectrometer for measurements.

2.4. Temperature-programmed surface reaction

Temperature-programmed surface reaction (TPSR) was carried out in a quartz tubular microreactor (i.d.

4 mm) containing 80 mg of Mn/HZSM-5 sample, using a HP G1800A mass spectrometer for product monitoring. The sample was pretreated in helium by heating from room temperature to $800\text{ }^\circ\text{C}$ at a rate of $15\text{ }^\circ\text{C min}^{-1}$, held at that temperature for 10 min and then cooled to room temperature. The gas was then switched to a reactant stream of 10 vol% methane in helium and the reactor then heated at the rate of $10\text{ }^\circ\text{C min}^{-1}$ from room temperature to $800\text{ }^\circ\text{C}$. Methane and the evolved products: CO , CO_2 , C_2H_4 , and C_6H_6 were continuously monitored at $m/e = 16, 28, 44, 26, 78$, respectively.

2.5. Temperature-programmed oxidation

The temperature-programmed oxidation (TPO) investigation was conducted with Mn/HZSM-5 samples (22 mg) which had been used for the methane aromatization reaction for 6 h at different temperatures. A sample was first heated at $120\text{ }^\circ\text{C}$ for 30 min and then cooled to room temperature in helium. It was then heated in an O_2/He mixture (8 vol% oxygen) from 40 to $800\text{ }^\circ\text{C}$ at a rate of $8\text{ }^\circ\text{C min}^{-1}$. The effluent from the reactor was analyzed online by mass spectrometry with an HP G1800A mass spectrometer.

3. Results and discussion

3.1. Thermal analysis

The DTA-TG profiles of the uncalcined 4 wt% Mn/HZSM-5 and manganese acetate tetrahydrate (MTA) are shown in figure 1. For MTA an initial endothermic weight loss at around $100\text{ }^\circ\text{C}$, corresponding to the lost of water of crystallization was observed. The manganese acetate formed was stable up to $250\text{ }^\circ\text{C}$, at which a drastic weight loss with two exothermic peaks was observed. We deduce that the first exothermic process was resulted from surface oxidation and the second from bulk oxidation of manganese acetate. The weight

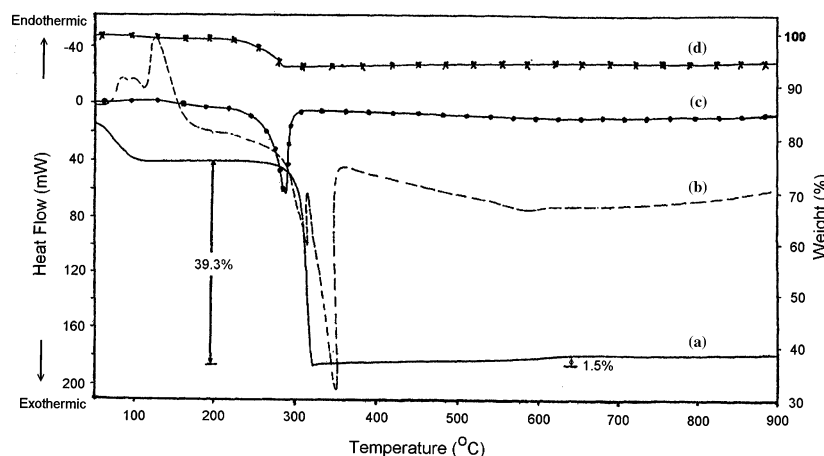
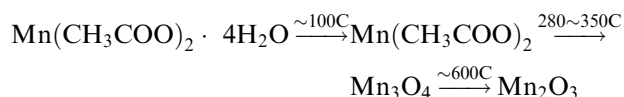


Figure 1. DTA-TG profiles of manganese acetate tetrahydrate (MTA) and uncalcined 4 wt% Mn/HZSM-5: (a) MTA, TG; (b) MTA-DTA; (c) uncalcined Mn/HZSM-5, DTA; (d) uncalcined Mn/HZSM-5, TG.

loss is attributed to the formation of Mn_3O_4 from manganese acetate since the observed weight lost of 39.3% is in close agreement with the predicted value of 39.5% for the process. A small exothermic peak with a slight weight increase (1.5%) at around 600 °C was associated with the transformation of Mn_3O_4 to manganic oxide. The reactions for these three stages are shown in the following scheme:



Similar changes were observed over the uncalcined 4 wt% Mn/HZSM-5 sample except that the decomposition temperature of manganese acetate was completed below 300 °C. The shift in decomposition temperature of manganese acetate in comparison to that of MAT is possibly due to its dispersion as minute clusters on the HZSM-5 crystals. The results of thermal analysis suggest that at the calcination temperature of 500 °C, the manganomanganic oxide formed and is the precursor of the active catalyst.

3.2. Methane aromatization over Mn/HZSM-5 catalyst

The catalytic performance of the 4 wt% Mn/HZSM-5 as a function of reaction temperature (T_r) at a reactant flow of 1600 mL h^{-1} g^{-1} is summarized in table 1 and figure 2. At $T_r = 700^\circ\text{C}$, the major gas phase products in the first 60 min of reaction were CO, CO_2 , and H_2O , and a trace of C_2 -hydrocarbon (mainly ethane) produced via the oxidative coupling reaction of methane, making use of the oxygen from the catalyst precursor.

Following this initial induction period, ethylene became the main C_2 -hydrocarbon and aromatic compounds appeared. The aromatic yield increased initially with reaction time and reached a maximum of 1.9% at a methane conversion of 2.1% after 2 h, followed by a moderate decrease to a nearly constant level. After 6 h on-stream, about 1.0% aromatic yield could be obtained. At the same time, the C_2 -hydrocarbon yield increased continuously with on-stream time. With a rise in T_r from 700 to 800 °C, the induction time shortened

and the maximum aromatics yield was observed at an earlier reaction time. C_2 -hydrocarbon and aromatics yields as well as $\text{C}_2\text{H}_4/\text{C}_2\text{H}_6$ ratio also increased with increasing reaction temperature. At $T_r = 800^\circ\text{C}$ and at 2 h on-stream time, 6.9% methane conversion, 6.3% aromatics, and 0.6% C_2 -hydrocarbon yields were observed; the $\text{C}_2\text{H}_4/\text{C}_2\text{H}_6$ ratio reached 5.3:1. However, at the higher temperature, the activity of the Mn/HZSM-5 catalyst became unsustainable. At $T_r = 750^\circ\text{C}$, the aromatics yield decreased from 4.0% at 2 h to 2.0% at 6 h while the C_2 -hydrocarbon yield increased only marginally from 0.4% to 0.5% during the same time period. At $T_r = 800^\circ\text{C}$, the catalyst deactivated completely for aromatization reaction after ca. 4 h. Both the C_2 -hydrocarbon yield and the $\text{C}_2\text{H}_4/\text{C}_2\text{H}_6$ ratio first increased and then drastically decreased. The highest C_2 -hydrocarbon yield was ca. 1% after 4 h.

3.3. Temperature-programmed surface reaction, and X-ray photoelectron spectroscopy

The result of the TPSR of 10% methane in helium over Mn/HZSM-5 is shown in figure 3). Methane consumption and CO_x (CO and CO_2) formation started at ca. 580 °C and CO_x evolution could be divided into three stages: (i) from 580 to 750 °C, CO_2 was the main carbon-containing products and three small peaks were observed at 600 °C, 650 °C, and 700 °C; (ii) from 750–800 °C, CO evolution became dominant while the evolution of CO_2 slowed down; and (iii) after ca. 10 min reduction at 800 °C, CO_2 production stopped completely. The evolution of ethylene and benzene started and increased monotonically with the time of reaction. At the same time CO evolution began to slow down. The TPSR results suggest that the production of high hydrocarbons must be preceded by the reduction of manganomanganic oxide.

The Mn 2p, O 1s, and C 1s spectra of the 4 wt% Mn/HZSM-5 catalysts before and after reaction with pure methane at 700 °C are shown in figure 4. Over the fresh sample, the peak at 641.8 eV is consistent with the expected binding energy (BE) of the Mn 2p_{3/2} electron of Mn_3O_4 [5]. The O 1s spectra showed a strong peak at 532.4 eV and a small one at 530.2 eV. The former can be

Table 1
Methane aromatization over 4 wt% Mn/HZSM-5 catalyst at different temperatures in the absence of an oxidant

Reaction temperature (°C)	CH ₄ Conversion (mol%)	Selectivity (mol%)					Yield (mol%)	
		C ₂ H ₄	C ₂ H ₆	C ₆ H ₆	C ₇ H ₈	C ₁₀ H ₈	C ₂	Aromatics
700	2.1	5.9	2.6	78.6	3.2	9.7	0.2	1.9
750	4.4	5.8	2.7	76.1	2.8	12.6	0.4	4.0
800	6.9	7.6	1.5	75.6	3.4	11.9	0.6	6.3

GHSV = 1600 mL h^{-1} g^{-1} and data were recorded 2 h after the start of reaction.

C₂: C₂H₄ + C₂H₆.

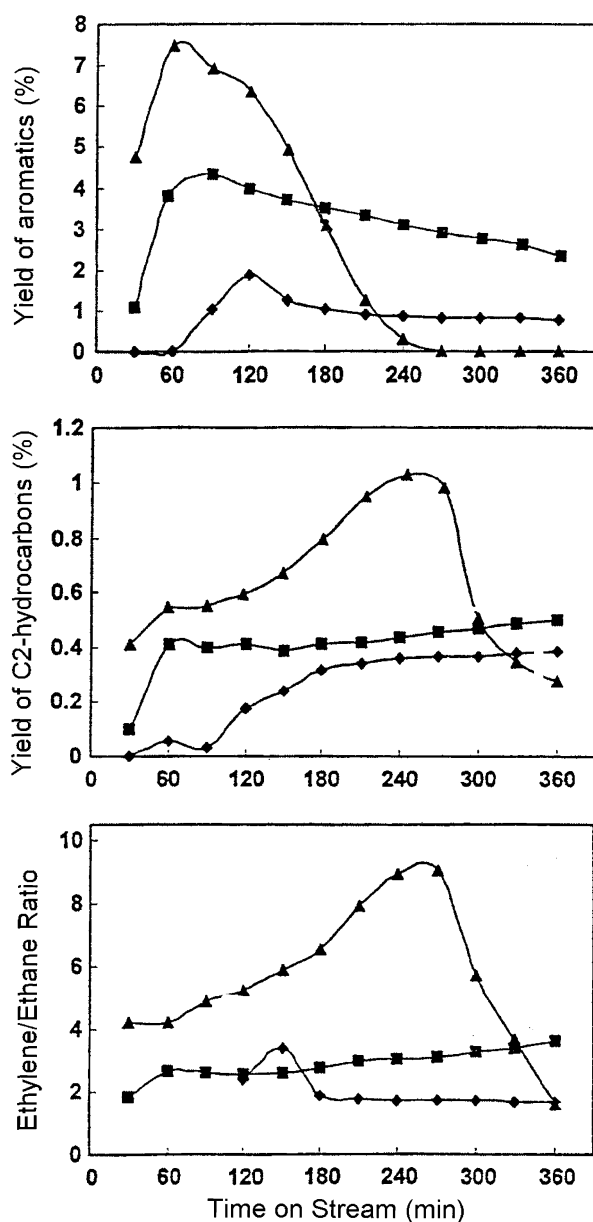


Figure 2. The catalytic performance of 4 wt% Mn/HZSM-5 catalyst at different temperature as a function of on-stream time. GHSV = $1600 \text{ mL h}^{-1} \text{ g}^{-1}$, \blacklozenge 700 °C, \blacksquare 750 °C, \blacktriangle 800 °C.

assigned to oxygen atoms of HZSM-5 zeolite [8], whereas the latter to Mn_3O_4 [5]. While it was reported that the binding energy of Mn $2p_{3/2}$ for different oxides of manganese varied by only a very small value, making it difficult to assign the oxidation state of Mn solely by binding energy [9], Fujiwara *et al.* [10] pointed out that a satellite peak with considerable intensity at a binding energy of ca. 5 eV higher than the corresponding main Mn $2p_{3/2}$ peak might denote the existence of manganese (II). In the used catalyst, a satellite peak at 647 eV developed, suggesting that reduction of manganese(IV) species possibly associated to manganese monoxide occurred during the methane

aromatization reaction. In addition, the 530.2 eV O 1s peak associated with manganese became very small and the main C1s signal broadened slightly and shifted from 284.4 to 283.9 eV.

3.4. Temperature-programmed oxidation

TPO-MS data obtained over the used 4 wt% Mn/HZSM-5 catalysts that had been used as catalyst at different temperatures (700–800 °C) are shown in figure 5. Over the 700 °C-reacted sample, CO_2 production started at about 310 °C, and four features were observed at 400, 480, 570, and 620 °C; the latter two were accompanied

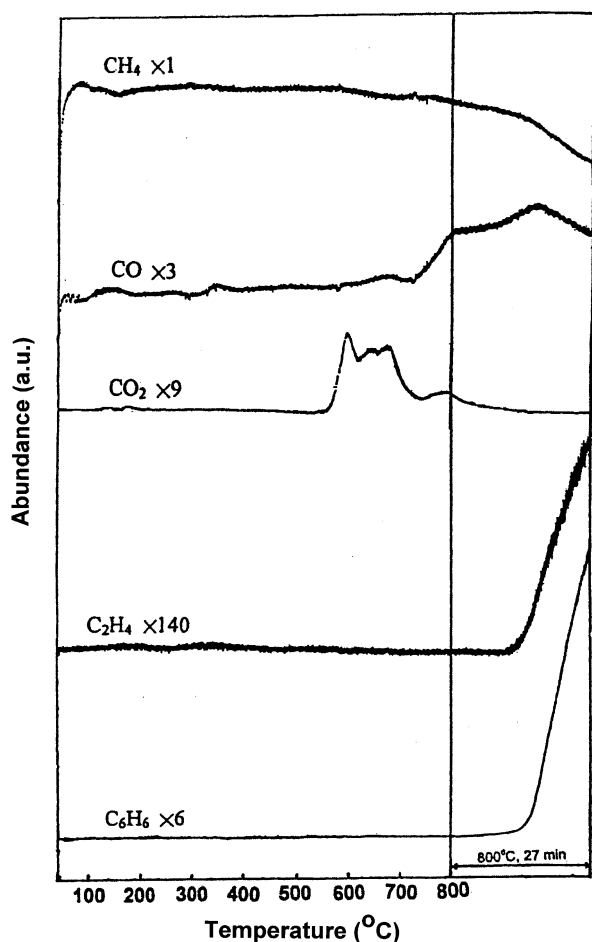


Figure 3. TPRS-MS profiles showing methane consumption and product evolution over 4 wt% Mn/HZSM-5 catalyst. Heating rate: $10\text{ }^{\circ}\text{C min}^{-1}$.

with water production, showing that the carbon species contained hydrogen. With T_r raised from 700 to 750 $^{\circ}\text{C}$, the amount of carbon oxidized at 400 $^{\circ}\text{C}$ decreased, whereas that at 490 $^{\circ}\text{C}$ carbon increased. Meanwhile, oxidation temperatures of the two hydrogenated cokes shifted to 610 and 660 $^{\circ}\text{C}$, respectively. At $T_r = 800\text{ }^{\circ}\text{C}$, three features were observed in the CO_2 production profile: a shoulder at ca. 490 $^{\circ}\text{C}$ and two broad ones at 580 and 660 $^{\circ}\text{C}$. Water peaks started at ca. 500 $^{\circ}\text{C}$. Carbon deposition on the catalyst surface increases with the temperature of the methane aromatization reaction. The amount of carbon burnt away as CO_x from the 750 $^{\circ}\text{C}$ and 800 $^{\circ}\text{C}$ reacted samples were 1.8 times and 3.5 times respectively that over the 700 $^{\circ}\text{C}$ reacted sample.

The nature of the coke deposited on catalysts by the methane aromatization reaction has been investigated with different methods. Using The UV-Raman spectroscopy, Ma et al. [11] detected a band at 1606 cm^{-1} with a broad shoulder at ca. 1400 cm^{-1} on Mo/HZSM-5 after reaction at 700 $^{\circ}\text{C}$. These were assigned to the C=C stretching mode from polyaromatic, substituted aromatic or even graphite species and to the C-H

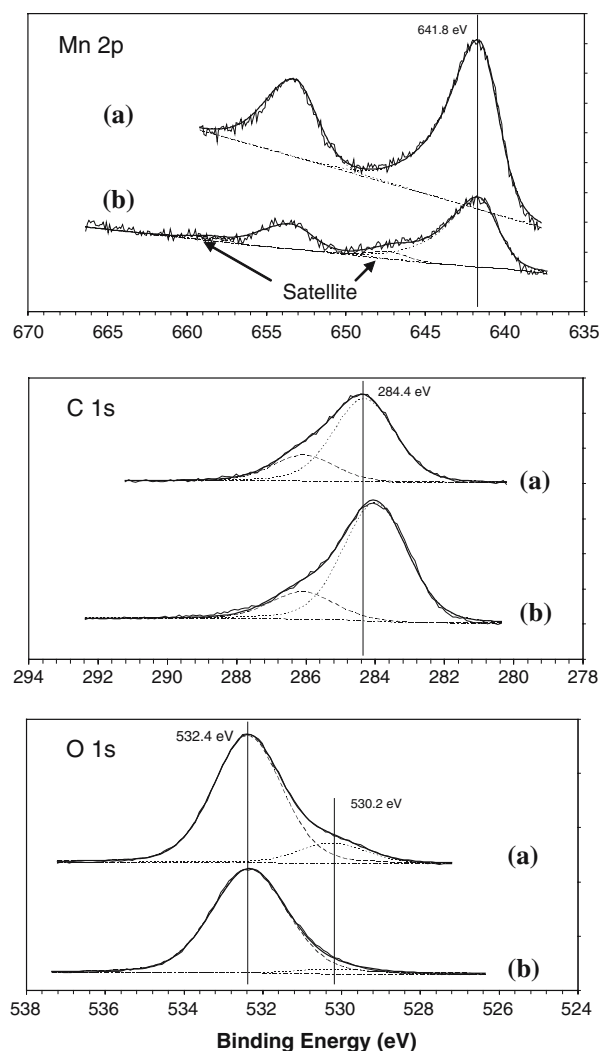


Figure 4. XPS spectra of 4 wt% Mn/HZSM catalysts: (a) before reaction (b) after reaction at 700 $^{\circ}\text{C}$ for 4 h.

bending mode of these coke species respectively. The absence of bands at about 3000 cm^{-1} indicated that there was no deposition of hydrogen-rich paraffinic coke [11]. Likewise we assigned the slightly hydrogenated cokes that burned off at 560 and 610 $^{\circ}\text{C}$ to polyaromatic species at two kinds of Brønsted acid sites [11]. In our previous study on Mo/HZSM-5, the carbonaceous depositions burned off at 490 $^{\circ}\text{C}$ without water could not be hydrogenated in temperature-programmed hydrogenation studies (TPH) [12] and was assigned to carbide [13]. Comparing the TPO results of Mn/HZSM-5 with those of Mo/HZSM-5, we deduce that on a used Mn/HZSM-5, the unhydrogenated carbon species that burnt off at around 400 and 480 $^{\circ}\text{C}$ is related to the manganese oxy-carbide or carbide.

3.5. Active phase for methane activation

Based on results of XPS and ^{13}C NMR studies, Sexton et al. [14] reported that during methanol

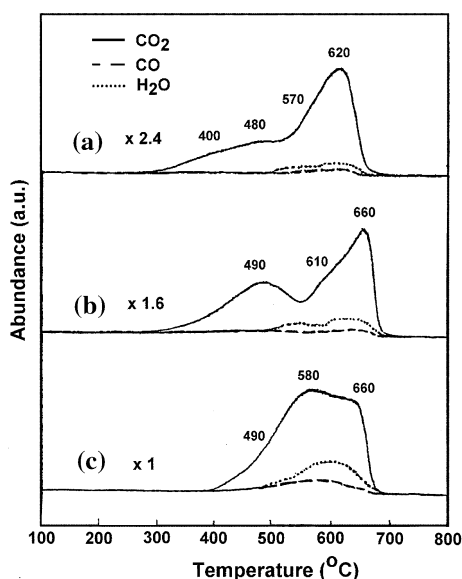


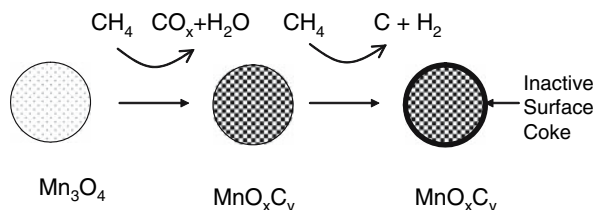
Figure 5. TPO-MS profiles of the products of oxidation of the carbonaceous species deposited on the 4 wt% Mn/HZSM-5 catalysts after 6 h of reaction at different temperature. (a) 700 °C, (b) 750 °C, (c) 800 °C.

conversion to aromatic compounds over ZSM-5, internal aromatic coke with a higher C 1s binding energy (284.7 eV) predominated until the catalyst was essentially deactivated; then external coke with a smaller C 1s BE (284.3 eV) which was graphitic or composed of highly condensed polyaromatics was formed. Solymosi *et al.* [15] observed similar BE shift of C 1s to 283.7 eV and broadening of the C 1s peak over Mo/HZSM-5 during methane aromatization and attributed this shift to the mixture of carbon species including carbidic carbon (283.3 eV), polymeric carbon (284.5 eV), and amorphous/graphitic carbon (285.0 eV). Our reaction results (figure 2) showed that at the reaction temperature of 800 °C, coke formation over Mn/HZSM-5 first suppressed ethylene oligomerization and cyclization at the acid sites that located mainly (>96%) inside the zeolite channels [16, 17], resulting in an increase in C₂H₄/C₂H₆ ratio and C₂-hydrocarbon yield at the expense of aromatics yield. Further coking on Mn sites led to complete deactivation of the catalyst for methane dehydrogenation and C₂-hydrocarbon formation. The relatively stable aromatics and C₂-hydrocarbon yields with time on-stream after the induction period at 700 °C suggested that coke formation on Mn sites was not severe at this temperature. Therefore, we argue that the shift in the binding energy of surface C 1s shown in figure 4 was due to carburization of Mn₃O₄. At 700 °C Mn carburization was not complete. Although the O 1s signal associated with Mn was diminished, it was not completely removed. We suggest that partially carburized Mn species, i.e. MnO_xC_y, with low carbon burnt off temperatures was formed on 700 °C-reacted Mn/HZSM-5 and was responsible for methane activation.

Raising the reaction temperature to 800 °C could lead to further carburization of the oxycarbide to carbide as reflected in the rise in the carbon burnt-off temperature. In the TPRS study, the formation of benzene was observed to continue at an increasing rate even when CO production started to diminish. If the drop in CO production is taken to indicate the depletion of oxygen, such depletion did not lower the rate of aromatic generation. This suggests that the carbide is also active and the deposition of excessive inactive coke is probably the cause of the eventual deactivation of the catalyst.

4. Conclusion

XPS and TPO results suggest the formation of carburized Mn species over the catalyst during the aromatization reaction. The carburized manganese is the active phase for catalytic methane aromatization whereas the oxide precursor can only produce C₂ hydrocarbons. The evolution of the manganese species over Mn/HZSM-5 during methane aromatization can be represented in the following scheme:



Hence an induction period was required before aromatic products could be formed when Mn/HZSM-5 catalyst was prepared by impregnation of HZSM-5 with manganese acetate tetrahydrate and then calcination at 500 °C, which produced Mn₃O₄ supported on the zeolite. The induction period can be shortened by raising the reaction temperature from 700 to 800 °C but this also hastened the complete deactivation of the catalyst.

Acknowledgments

The work described above was supported by a grant (FRG/99-00/II-25) from Hong Kong Baptist University. Pinglian Tan thanks the HKBU for a Ph. D. studentship.

References

- [1] D. Ma, Y. Shu, M. Cheng, Y. Xu and X. Bao, *J. Catal.* 194 (2000) 105.
- [2] B.M. Weckhuysen, D. Wang, M.P. Rosynek and J.H. Lunsford, *J. Catal.* 175 (1998) 338.
- [3] L. Wang, L. Tao, M. Xie, X. Guo, J. Huang and Y. Xu, *Catal. Lett.* 21 (1993) 35.

- [4] T. Inui, Y. Ishihara, K. Kamachi and H. Matsuda, *Zeolite: Facts, Figures, Future* (Elsevier Science Publishers, B.V., 1989) 1183.
- [5] L.M. Ioffe, P. Bosch, T. Viveros, H. Sanchez and Y.G. Borodko, *Mater. Chem. Phys.* 51 (1997) 269.
- [6] M. Marczewski and H. Marczewska, *Polish J. Chem.* 69 (1995) 956.
- [7] S. Li, C.-L. Zhang, Y. Yuan, T.-H. Wu, Z.-S. Xu and L.-W. Lin, *Gaodeng Xuexiao Huaxue Xuebao* 19 (1998) 964.
- [8] P.L. Tan, Y.L. Leung, C.T. Au and S.Y. Lai, *Appl. Catal. A* 228 (2002) 115.
- [9] B.R. Strohmeier and D.M. Hercules, *J. Phys. Chem.* 88 (1984) 4922.
- [10] M. Fujiwara, T. Matsushita and S. Ikeda, *J. Electron Spectrosc. Relat. Phenom.* 74 (1995) 201.
- [11] D. Ma, Y. Lu, L. Su, Z. Xu, Z. Tian, Y. Xu, L. Lin and X. Bao, *J. Phys. Chem.* 106 (2002) 8524.
- [12] P.L. Tan, K.W. Wong, C.T. Au and S.Y. Lai, *Appl. Catal. A* 253 (2003) 305.
- [13] H. Liu, T. Li, B. Tian and Y. Xu, *Appl. Catal. A* 213 (2001) 103.
- [14] B.A. Sexton, A.E. Hughes and D.M. Bibby, *J. Catal.* 109 (1988) 126.
- [15] F. Solymosi, J. Cserenyi, A. Szoke, T. Bansagi and A. Dszko, *J. Catal.* 165 (1997) 150.
- [16] L. Wang and W.K. Hall, *J. Catal.* 77 (1982) 232.
- [17] W. Zhang, D. Ma, X. Han, X. Liu, X. Bao, X. Guo and X. Wang, *J. Catal.* 188 (1999) 393.